Supplement of Atmos. Chem. Phys., 24, 10279–10304, 2024
https://doi.org/10.5194/acp-24-10279-2024-supplement

Atmospheric Chemistry and Physics
Open Access
EGU

Supplement of

Biomass-burning sources control ambient particulate matter, but traffic and industrial sources control volatile organic compound (VOC) emissions and secondary-pollutant formation during extreme pollution events in Delhi

Arpit Awasthi et al.

Correspondence to: Baerbel Sinha (bsinha@iisermohali.ac.in)

Table S1: 111 NMVOCs species used in the PMF model, the table lists the major compound identifications and the references supporting such assignments from previous works, along with average of the observational period reported in this study (with range min-max), detection limits, precision error.

m/z (H+)	Potential contributor	Strong /Weak	average (with range) µg/m^3	Detection limit µgm^{-3}	Precision error (%)	Sources	References
31.014	Formaldehyde HCHO	Strong	1.063 (0.066-9.464)	0.024	3.7	Photochemical production, traffic, biomass burning	Hatch et al., 2015; Stockwell et al., 2015; Koss et al., 2018
33.030	Methanol CH_3OH	Strong	17.285 (3.522-127.853)	0.038	2.1	Photochemical production, biomass burning, biogenic	Hatch et al., 2015; Stockwell et al., 2015; Koss et al., 2018
41.035	Propyne C_3H_4	Strong	9.149 (1.001-96.661)	0.041	2.1	Traffic, biomass burning	Hatch et al., 2015; Stockwell et al., 2015; Koss et al., 2018; Hakkim et al., 2021
42.030	Acetonitrile C_2H_3N	Strong	0.888 (0.208-5.208)	0.003	4.3	Biomass burning, industries	Hatch et al., 2015; 2017
43.051	Propene C_3H_6	Strong	5.117 (0.766-59.931)	0.027	2.8	Biomass burning, traffic	Hakkim et al., 2021
44.018	Isocyanic acid HNCO	Strong	0.145 (0.007-1.231)	0.007	10.5	Oxidation of amines (secondary formation), biomass burning	Chandra & Sinha, 2016; Wang et al., 2020
45.030	Acetaldehyde CH_3CHO	Strong	8.764 (1.432-55.175)	0.059	1.5	Biogenic, biomass burning, photochemical production	Hatch et al., 2015; Stockwell et al., 2015. Koss et al., 2018; Kumar et al., 2021
46.025	Formamide CH_3NO	Strong	0.447 (0.004-8.3)	0.012	6	Oxidation of amines (secondary formation)	Yao et al., 2016; Wang et al., 2022
47.009	Formic acid HCOOH	Strong	1.717 (0.004-31.063)	0.055	4.2	Oxidation of amines (secondary formation)	Yao et al., 2016; Wang et al., 2022
47.0457	Ethanol C_2H_6O	Strong	0.625 (0.052-7.845)	0.002	5.8	Industrial, Traffic	Bruns et al., 2017; Koss et al., 2018
48.048	Methoxyamine CH_5NO	Weak	0.011 (0-0.148)	0.001	39.6	Oxidation of amines (secondary formation)	Yáñez-Serrano et al., 2021
49.007	Methanethiol CH_4S	Strong	0.15 (0.002-3.295)	0.002	15.4	Industrial	Toda et al., 2010
53.035	Vinylacetylene, 1-Buten-3-yne C_4H_4	Strong	0.662 (0.003-10.879)	0.007	6.3	Biomass burning	Hatch et al., 2015; Stockwell et al., 2015; Koss et al., 2018
55.051	1,2-Butadiene, 1-Butyne, 2-Butyne, 1,3 Butadiene C_4H_6	Strong	3.701 (0.418-30.204)	0.029	3.5	Biomass burning	Koss et al., 2018; Sarkar et al., 2017
57.030	Acrolein C_3H_4O	Strong	0.802 (0-8.038)	0.012	5.7	Biomass burning, waste burning	Kumar et al., 2021
57.067	Methyl tert-butyl ether (MTBE) fragment /Butene C_4H_8	Strong	7.293 (0.983-100.664)	0.024	2.5	Biomass burning, waste burning, traffic	Hakkim et al., 2021
59.046	Acetone + Propanal	Strong	14.603	0.016	2.4	Biomass burning,	Hatch et al., 2015;

	C_3H_6O		(2.341-145.458)			industries, photochemical production	Stockwell et al., 2015; Koss et al., 2018; Kumar et al., 2021
61.025	Acetic acid+ Glycolaldehyde $C_2H_4O_2$	Strong	16.086 (0.695-170.723)	0.033	1.9	Photochemical production, biomass burning, industries	Kumar et al., 2021
62.997	Vinyl chloride C_2H_3Cl	Weak	0.02 (0.001-0.235)	0.001	37.1	PVC burning	Hsu et al., 2022; Fukusaki et al., 2021
67.051	Cyclopentadiene, monoterpene fragment, butanol fragment C_5H_6	Strong	0.781 (0.117-10.93)	0.01	8.2	Biomass burning	Hatch et al., 2015; Stockwell et al., 2015
69.031	Furan C_4H_4O	Strong	0.231 (0.011-3.247)	0.006	11.5	Biomass burning	Coggon et al., 2019; Hatch et al., 2015; 2017; Koss et al., 2018; Stockwell et al., 2015
69.067	Isoprene + 2-methyl-3-butene-2-ol fragment C_5H_8	Strong	2.234 (0.294-17.733)	0.014	4.9	Biogenic sources, biomass burning	Stockwell et al., 2015; Jordan et al., 2009
71.047	Methyl Vinyl Ketone, Methacrolein, Butenal C_4H_6O	Strong	1.015 (0.099-4.729)	0.013	5.6	Biomass burning, photochemical production	Stockwell et al., 2015; de Gouw et al., 2007
73.026	Methylglyoxal $C_3H_4O_2$	Strong	0.56 (0.004-8.797)	0.024	8.6	Oxidation of amines (secondary formation)	Yao et al., 2016; Wang et al., 2022
73.062	Butanal, butanone, MEK C_4H_8O	Strong	2.534 (0.315-43.128)	0.006	3.6	Biomass burning, biogenic, photochemical production	Hatch et al., 2015; Stockwell et al., 2015; Koss et al., 2018
75.042	Hydroxyacetone, propanoic acid $C_3H_6O_2$	Strong	1.664 (0.116-14.045)	0.005	8.5	Biomass burning, biogenic, traffic	Kumar et al., 2021
76.037	Nitroethane $C_2H_5NO_2$	Strong	0.036 (0.002-0.308)	0.013	5.4	Biomass burning	Palm et al., 2020, Harrison et al., 2005
79.052	Benzene C_6H_6	Strong	6.07 (0.305-68.694)	0.007	1.7	Biomass burning, traffic	Hatch et al., 2015; Stockwell et al., 2015; Koss et al., 2018; Hakkim et al., 2021
81.031	Cyclopentadienone C_5H_4O	Strong	0.102 (0.001-0.896)	0.004	17.3	Biomass burning	Hatch et al., 2015; Koss et al., 2018; Nowakowska et al., 2018
83.047	Methyl furan C_5H_6O	Strong	0.363 (0.032-3.68)	0.018	10.2	Biomass burning	Coggon et al., 2019; Hatch et al., 2015; 2017; Koss et al., 2018; Stockwell et al., 2015
83.084	Cyclohexene, hexyne isomers C_6H_{10}	Strong	1.406 (0.345-12.044)	0.007	6.6	Biomass burning, biogenic, traffic	Stockwell et al., 2015; Koss et al., 2018; Kumar et al., 2021
84.080	Pentanenitrile. methylbutanenitrile isomers, C5-amines C_5H_9N	Strong	0.037 (0-0.495)	0.011	28.7	Biogenic, biomass burning	Hatch et al., 2015; 2017
85.027	Furanone, butenedial $C_4H_4O_2$	Strong	0.466 (0.015-6.719)	0.002	6.4	Biomass burning, photochemical production	Coggon et al., 2019; Hatch et al., 2015; 2017; Koss et al., 2018; Stockwell et al., 2015
85.063	Cyclopentanone C_5H_8O	Strong	0.337 (0.042-1.971)	0.025	10.4	Biomass burning, traffic	Hatch et al., 2015; Koss et al., 2018;

							Nowakowska et al., 2018
85.094	Cyclohexane, Hexene C_6H_{12}	Strong	0.326 (0.051-4.057)	0.009	12.7	Biomass burning, Traffic	Fleming et al., 2018; Hakkim et al., 2021
87.043	Isomers of C4 carboxylic acid/ester/diketone $C_4H_6O_2$	Strong	1.118 (0.06-8.545)	0.006	6.7	Biomass burning, photochemical production	Kumar et al., 2021[Hatch et al., 2015; Koss et al., 2018; Nowakowska et al., 2018
87.079	Pentanone, methyl-buteneol, pentanal $C_5H_{10}O$	Strong	0.295 (0.05-1.841)	0.023	11.6	Biomass burning, biogenic	Hatch et al., 2015; Stockwell et al., 2015; Koss et al., 2018
89.058	Isomers of C4-carboxylic acidester $C_4H_8O_2$	Strong	1.306 (0.087-17.301)	0.003	6.1	Industrial solvent	Kamarulzaman et al., 2019
91.053	Monoterpene fragment C_7H_6	Strong	1.24 (0.058-20.618)	0.008	5.9	Industrial, Traffic	Kamarulzaman et al., 2019
93.069	Toluene C_7H_8	Strong	18.285 (0.43-321.651)	0.004	1.7	Biomass burning traffic, chemical production, biogenic	Hatch et al., 2015; Stockwell et al., 2015; Koss et al., 2018; Hakkim et al., 2021
95.048	Phenol C_6H_6O	Strong	0.835 (0.069-9.968)	0.023	6.1	Biomass burning, photochemical production	Hakkim et al., 2021; Koss et al., 2018; Kumar et al., 2021
95.084	Monoterpene fragment C_7H_{10}	Strong	0.826 (0.111-13.348)	0.008	9	Industrial, traffic	Kamarulzaman et al., 2019
97.027	Furfural, isomers of diketone, carboxylic acid / ester $C_5H_4O_2$	Strong	0.649 (0.026-17.29)	0.013	9.5	Biomass burning	Kumar et al., 2021; Coggon et al., 2019; Hatch et al., 2015; 2017; Koss et al., 2018; Stockwell et al., 2015
97.063	C2 substituted furan, methyl Cyclopentenone C_6H_8O	Strong	0.277 (0.024-2.555)	0.008	12.2	Biomass burning	Coggon et al., 2019; Hatch et al. 2015; 2017; Koss et al., 2018; Stockwell et al., 2015
97.100	Cycloheptene, alkyl fragment C_7H_{12}	Strong	0.634 (0.104-7.483)	0.011	10.1	Biomass burning	Stockwell et al., 2015; Koss et al., 2018; Kumar et al., 2021
99.043	Furfuryl alcohol, Methyl-furanone $C_5H_6O_2$	Strong	0.599 (0.025-4.61)	0.009	9.5	Photochemical production, Biomass burning	Coggon et al., 2019; Hatch et al., 2015; 2017; Koss et al., 2018; Stockwell et al., 2015
99.079	Cyclohexanone, isomers of C6-aldehyde/ketone $C_6H_{10}O$	Strong	1.033 (0.088-23.49)	0.022	8.3	Industrial	Gupta et al., 1979
99.116	Methylcyclohexane, heptene & other hydrocarbons C_7H_{14}	Weak	0.034 (0.002-0.472)	0.012	42.6	asphalt degassing	Khare et al., 2020
101.059	Pentanedione, isomers of C5-diketone/ carboxylic acid/ ester/ aldehyde $C_5H_8O_2$	Strong	0.777 (0.048-5.073)	0.002	8.5	Biomass burning	Hatch et al., 2015; Koss et al. 2018; Nowakowska et al., 2018
105.069	Styrene C_8H_8	Strong	1.556 (0.13-35.843)	0.021	7	Biomass burning traffic, chemical production	Jordan et al., 2009; Stockwell et al., 2015
107.050	Benzaldehyde, isomers of C7-aldehyde/ ketone C_7H_6O	Strong	0.484 (0.003-4.687)	0.004	9.7	Biomass burning, photochemical production	Hatch et al., 2015; Stockwell et al., 2015; Koss et al., 2018

107.085	Sum of C8-Aromatics C_8H_{10}	Strong	11.214 (0.4-193.065)	0.004	2.6	Biomass burning, traffic	Hatch et al., 2015; Stockwell et al., 2015; Koss et al., 2018; Hakkim et al., 2021
109.064	Methylphenol isomers, Anisole C_7H_8O	Strong	0.24 (0.021-2.61)	0.005	14.1	Biomass Burning	Hatch et al., 2015
109.100	Terpene fragment/Cyclooctadiene C_8H_{12}	Strong	0.511 (0.089-5.681)	0.006	11.8	Industrial, traffic	Kamarulzaman et al., 2019
111.042	Methylfurfural, Hydroxyphenol $C_6H_6O_2$	Strong	0.208 (0.002-4.11)	0.009	16	Biomass burning, photochemical production	Coggon et al., 2019; Hatch et al., 2015; 2017; Koss et al., 2018; Stockwell et al., 2015
111.080	C3-substituted furans, C2-substituted cyclopentene, methyl cyclohexene $C_7H_{10}O$	Strong	0.195 (0.024-1.519)	0.016	15.5	Biomass burning	Coggon et al., 2019; Hatch et al. 2015; 2017; Koss et al., 2018; Stockwell et al., 2015
111.116	Ethenyl cyclohexane C_8H_{14}	Strong	0.434 (0.078-5.193)	0.005	12.6	Ring-opening products of cyclic alkanes	Wang et. al., 2015
113.059	Dimethylbutenedial, C4-substituted aldehyde $C_6H_8O_2$	Strong	0.403 (0.023-2.736)	0.009	11.8	Oxidation of aromatic compounds, biomass burning	Zaytsev et al., 2019
115.039	Hydroxymethyl furanone, methylepoxybutanedial $C_5H_6O_3$	Strong	0.119 (0.004-1.797)	0.012	18.8	Photochemical production, Biomass burning	Coggon et al., 2019; Hatch et al. 2015; 2017; Koss et al., 2018; Stockwell et al., 2015
115.075	Isomers of C6-diketones, aldehyde, caroboxylic acid/ester $C_6H_{10}O_2$	Strong	0.357 (0.024-2.187)	0.013	12.7	Oxidation of polyaromatic hydrocarbons	Bruns et al., 2017
116.108	C6-amides $C_6H_{13}NO$	Weak	0.035 (0-0.255)	0.012	34.2	Photooxidation of amines	Yao et al., 2016
119.085	Terpene fragment C_9H_{10}	Strong	0.608 (0.062-9.105)	0.001	9.3	Traffic	Erickson et al., 2013
121.064	Tolualdehyde, isomers of C8-aldehyde, ketone C_8H_8O	Strong	0.578 (0.048-6.186)	0.004	9.4	Biomass burning	Hatch et al., 2015; Koss et al., 2018
121.101	Sum of C-9 aromatics C_9H_{12}	Strong	5.67 (0.174-125.472)	0.004	3.5	Traffic, Biomass burning	Hatch et al., 2015; Stockwell et al., 2015; Koss et al., 2018
123.044	Hydroxybenzaldehyde/isomers of C7- carboxylic acid/ ester $C_7H_6O_2$	Strong	0.307 (0.009-2.77)	0.004	13.6	Photochemical production, Biomass burning	Hatch et al., 2015; Koss et al., 2018; Nowakowska et al., 2018
123.080	C2-substituted phenol, methyl anisole $C_8H_{10}O$	Strong	0.146 (0.013-1.255)	0.006	18.6	Oxidation of polyaromatic hydrocarbons	Bruns et al., 2017
123.12	Santene, Cyclopentadiene & other hydrocarbons C_9H_{14}	Strong	0.349 (0.063-3.73)	0.009	14.6	asphalt degassing	Khare et al., 2020; Kılıç et al., 2018
124.039	Nitrobenzene $C_6H_5NO_2$	Strong	0.054 (0.004-0.871)	0.002	25.3	Traffic	Palm et al., 2020; Harrison et al., 2005
125.060	Guaiacol, isomers of C7-carboxylic acid/ester	Strong	0.162 (0.01-2.15)	0.009	19.2	Biomass burning	Hatch et al., 2015; Koss et al., 2018;

	$C_7H_8O_2$						Nowakowska et al., 2018
125.133	Nonyne, nondiene C_9H_{16}	Strong	0.157 (0.033-1.702)	0.005	21.4	asphalt degassing	Khare et al., 2020; Kılıç et al., 2018
127.039	Hydroxymethyl furfural $C_6H_6O_3$	Strong	0.116 (0.004-2.045)	0.01	18.9	biomass burning	Koss et al., 2018
127.075	Isomers of C7-carboxylic acid/ ester/ aldehdyde/ ketone $C_7H_{10}O_2$	Strong	0.226 (0.014-1.5)	0.013	16.3	Oxidation of aromatic compounds, biomass burning	Zaytesv et al., 2019
129.070	Naphthalene $C_{10}H_8$	Strong	1.043 (0.099-12.618)	0.012	8.7	Traffic, biomass burning	Hakkim et al., 2021; Koss et al., 2018; Kumar et al., 2021
129.092	Isomers of C9-acetaldehyde/ ketone/ carboxylic acid/ ester $C_7H_{12}O_2$	Strong	0.176 (0.01-1.274)	0.006	18.2	Oxidation of polyaromatic hydrocarbons	Bruns et al., 2017; Lignell et al., 2013
133.065	Methyl benzofuran C_9H_8O	Strong	0.078 (0.007-0.617)	0.003	26.7	Biomass Burning	Hatch et al., 2015
133.102	Ethyl styrene, tetrahydronaphthalene $C_{10}H_{12}$	Strong	0.457 (0.044-7.886)	0.003	13.4	Traffic	Yáñez-Serrano et al., 2021
135.080	Isomers of C9-acetaldehyde/ ketone $C_9H_{10}O$	Strong	0.172 (0.007-1.367)	0.004	17.9	Traffic	Knighton et al., 2007
135.118	P-cymene, C4-substituted benzene, C2-substituted xylene $C_{10}H_{14}$	Strong	2.509 (0.091-71.697)	0.005	5.7	Traffic	Hakkim et al., 2021
137.133	Sum of Monoterpenes (MT) $C_{10}H_{16}$	Strong	2.66 (0.167-127.676)	0.006	10.3	Industrial, biogenic, biomass burning, traffic	Guenther et al., 2006; Kamarulzaman et al., 2019; Koss et al., 2018; Kumar et al., 2021
138.056	Nitrotoluene/ salicylamide $C_7H_7NO_2$	Weak	0.036 (0.001-0.707)	0.003	32.9	Oxidation of toluene	Ramasamy et al., 2019
143.086	Methyl naphthalene $C_{11}H_{10}$	Strong	0.19 (0.015-2.848)	0.004	21.2	Biomass Burning, Traffic	Hatch et al., 2015; Yáñez-Serrano et al., 2021
143.108	Isomers of C8-aldehyde/ketone/carboxylic acid /ester $C_8H_{14}O_2$	Strong	0.153 (0.022-0.942)	0.011	20.7	Oxidation of polyaromatic hydrocarbons	Bruns et al., 2017
145.051	Organic acids/ levoglucosan fragment $C_6H_8O_4$	Strong	0.068 (0.002-1.626)	0.009	27.2	Biomass Burning	Hatch et al., 2015; Koss et al., 2018; Nowakowska et al., 2018
145.102	C2-substituted indene $C_{11}H_{12}$	Weak	0.062 (0.007-0.814)	0.004	36.7	Asphalt degassing	Khare et al., 2020
145.123	Isomer of C8-carboxylic acid/ C8-ester $C_8H_{16}O_2$	Strong	0.072 (0.003-0.96)	0.004	29.3	Oxidation of polyaromatic hydrocarbons	Bruns et al., 2017; Mochizuki et al., 2019
146.977	Isomers of dichlorobenzene $C_6H_4Cl_2$	Strong	0.352 (0.009-5.79)	0.001	13.7	Industrial pesticides	Graus et al., 2010; Yáñez-Serrano et al., 2021
147.118	Cyclopentylbenzene & other hydrocarbons $C_{11}H_{14}$	Strong	0.318 (0.038-4.599)	0.002	16.7	asphalt degassing	Khare et al., 2020
149.024	Phthalic anhydride, benzofurandione $C_8H_4O_3$	Strong	0.195 (0.003-4.508)	0.007	15.3	Oxidation of polyaromatic hydrocarbons	Bruns et al., 2017

149.096	Isomers of C10-aldehyde/ ketone $C_{10}H_{12}O$	Strong	0.094 (0.008-1.25)	0.003	26.4	asphalt degassing	Khare et al., 2020
153.092	Isomers of C9-carboxylic acid/ester $C_9H_{12}O_2$	Strong	0.102 (0.01-1.413)	0.01	25.3	Oxidation of monoterpenes	Gkatzelis et al. 2018
153.128	Isomers of C10-aldehyde/ ketone $C_{10}H_{16}O$	Strong	0.31 (0.021-7.93)	0.005	15.2	Oxidation of monoterpenes	Camredon et al., 2010
154.052	Nitrobenzyl alcohol/ Nitrocresols, methyl-nitrophenol $C_7H_7NO_3$	Strong	0.077 (0.003-0.577)	0.003	27.5	Oxidation of toluene	Ramasamy et al., 2019
155.108	Isomers of C9-ketone/ C9-carboxylic acid/ C9-ester $C_9H_{14}O_2$	Strong	0.104 (0.008-0.759)	0.009	25.5	Oxidation of monoterpenes	Camredon et al.:,2010; Gkatzelis et al., 2018
155.144	Isomers of C10-aldehyde/ ketone $C_{10}H_{18}O$	Strong	0.092 (0.008-1.238)	0.005	26.7	asphalt degassing	Khare et al., 2020
157.099	C2-substituted naphthalene $C_{12}H_{12}$	Strong	0.144 (0.017-1.209)	0.005	23.9	asphalt degassing	Khare et al., 2020; Kılıç et al., 2018
157.122	C9-ester/ C9-organic acid $C_9H_{16}O_2$	Strong	0.109 (0.012-1.035)	0.02	23.6	Oxidation of monoterpenes	Lignell et al., 2013; Camredon et al., 2010
159.140	C9-organic acid $C_9H_{18}O_2$	Weak	0.056 (0.002-0.559)	0.005	32.8	Oxidation of monoterpenes	Mochizuki et al., 2019
161.134	Cyclohexylbenzene, butyl styrene, cyclopentylmethylbenzene $C_{12}H_{16}$	Strong	0.161 (0.016-2.527)	0.002	24.1	asphalt degassing	Khare et al., 2020; Kılıç et al., 2018
175.150	Trimethyltetralin/ ionene $C_{13}H_{18}$	Strong	0.086 (0.007-1.677)	0.001	33.6	asphalt degassing	Khare et al., 2020
177.056	Formylcinnamic acid / hydroxy-methyl-coumarin $C_{10}H_8O_3$	Strong	0.105 (0.006-0.852)	0.004	25.9	asphalt degassing	Xing et al., 2023
177.165	C7-substituted benzene, $C_{13}H_{20}$	Strong	0.13 (0.013-2.594)	0.003	27.8	asphalt degassing	Khare et al., 2020
179.181	C3-substituted adamantane $C_{13}H_{22}$	Weak	0.06 (0.006-0.878)	0.003	38.5	asphalt degassing	Khare et al., 2020
183.121	Bibenzyl $C_{14}H_{14}$	Weak	0.029 (0.004-0.2)	0.004	58.5	asphalt degassing	Khare et al., 2020
185.121	cis-Pinonic acid / C10-ester $C_{10}H_{16}O_3$	Weak	0.054 (0.007-1.571)	0.006	35.2	Oxidation of monoterpenes	Camredon et al., 2010
187.148	C4-substituted dihydroazulene, benzyl cycloheptene $C_{14}H_{18}$	Weak	0.039 (0.005-0.306)	0.006	47.7	asphalt degassing agriculture	Khare et al., 2020; Loubet et al., 2022
189.165	C4-substituted dihydronaphthalene cyclopentylpropyl benzene $C_{14}H_{20}$	Weak	0.053 (0.006-0.818)	0.002	43.5	asphalt degassing	Khare et al., 2020
191.181	C8-substituted benzene	Weak	0.068	0.002	38.1	asphalt degassing	Khare et al., 2020

	$C_{14}H_{22}$		(0.007-0.892)				
195.138	Myrtenyl acetate/C12-organic acid/C12-ester $C_{12}H_{18}O_2$	Weak	0.029 (0.003-0.766)	0.005	48.4	Oxidation of biomass burning	Haeri, 2023
217.195	C6-substituted dihydronaphthalene $C_{16}H_{24}$	Weak	0.026 (0.003-0.307)	0.002	63.1	asphalt degassing	Khare et al., 2020
233.228	C11-substituted benzene $C_{17}H_{28}$	Weak	0.023 (0.002-0.215)	0.002	67.1	asphalt degassing organic aerosol	Khare et al., 2020, Xu et al., 2022
247.243	C12-substituted benzene $C_{18}H_{30}$	Weak	0.022 (0.002-0.158)	0.004	66	asphalt degassing	Khare et al., 2020

Table S2: List of Constraints incorporated in the PMF model

Factor	Element	Type
Biogenic	m/z 42.030	Pull Down Maximally
Biogenic	m/z 93.069	Pull Down Maximally
Biogenic	m/z 107.085	Pull Down Maximally
Biogenic	m/z 121.101	Pull Down Maximally
Biogenic	10/16/2022 11:00:00 PM	Pull Down Maximally
Biogenic	10/17/2022 1:00:00 AM	Pull Down Maximally
Biogenic	10/17/2022 12:00:00 AM	Pull Down Maximally
Biogenic	10/17/2022 2:00:00 AM	Pull Down Maximally
Biogenic	10/16/2022 10:00:00 PM	Pull Down Maximally
Biogenic	10/16/2022 9:00:00 PM	Pull Down Maximally
Biogenic	10/21/2022 10:00:00 PM	Pull Down Maximally
Biogenic	10/21/2022 11:00:00 PM	Pull Down Maximally
Biogenic	10/22/2022 12:00:00 AM	Pull Down Maximally
Biogenic	10/21/2022 9:00:00 PM	Pull Down Maximally
Biogenic	10/21/2022 8:00:00 PM	Pull Down Maximally
Biogenic	10/22/2022 6:00:00 PM	Pull Down Maximally
Biogenic	10/23/2022 7:00:00 PM	Pull Down Maximally
Biogenic	10/26/2022 11:00:00 PM	Pull Down Maximally
Photochemical	m/z 42.030	Pull Down Maximally
Photochemical	m/z 93.069	Pull Down Maximally

Photochemical	m/z 107.085	Pull Down Maximally
Photochemical	m/z 121.101	Pull Down Maximally
Photochemical	9/20/2022 2:00:00 AM	Pull Down Maximally
Photochemical	9/20/2022 11:00:00 PM	Pull Down Maximally
Photochemical	9/22/2022 1:00:00 AM	Pull Down Maximally
Photochemical	9/23/2022 10:00:00 PM	Pull Down Maximally
Photochemical	9/24/2022 1:00:00 AM	Pull Down Maximally
Photochemical	10/4/2022 2:00:00 AM	Pull Down Maximally
Photochemical	10/4/2022 4:00:00 AM	Pull Down Maximally
Cooking	10/17/2022 8:00:00 PM	Pull Up Maximally
Solvents	11/8/2022 4:00:00 AM	Pull Up Maximally
Road Construction	10/17/2022 9:00:00 PM	Pull Up Maximally
Petrol 4-Wheeler	10/18/2022 11:00:00 PM	Pull Up Maximally
Paddy	11/12/2022 1:00:00 AM	Pull Up Maximally
Paddy	11/12/2022 12:00:00 AM	Pull Up Maximally
Heating & Waste Disposal	11/19/2022 11:00:00 PM	Pull Up Maximally
Petrol 2-Wheeler	10/17/2022 9:00:00 PM	Pull Up Maximally
Industrial	10/16/2022 11:00:00 PM	Pull Up Maximally
CNG	10/16/2022 7:00:00 PM	Pull Up Maximally

Table S3: Contains the SOA yields for 53 compounds to calculate the SOAP

m/z	SOAP	References
HCHO	0.7	Derwent et al., 2010
CH_3OH	0.3	Derwent et al., 2010
HCOOH	0.1	Derwent et al., 2010
C_2H_6O	0.6	Derwent et al., 2010
C_4H_6	30.6	Xiong et al., 2020
C_3H_4O	11.5	Hakkim et al., 2021
C_3H_6O	0.3	Derwent et al., 2010
$C_2H_4O_2$	0.1	Derwent et al., 2010
C_4H_4O	29.4	Hakkim et al., 2021
C_5H_8	42.3	Hakkim et al., 2021, Xiong et al., 2020
C_4H_6O	82.2	Hakkim et al., 2021
C_4H_8O	0.6	Derwent et al., 2010
C_6H_6	145.6	Chan et al., 2009, Kılıç et al., 2018, Hakkim et al., 2021, Xiong et al., 2020
C_5H_6O	41.2	Hakkim et al., 2021
C_6H_{13}	1	Xiong et al., 2020
$C_4H_9O_2$	0.1	Derwent et al., 2010
C_7H_8	100	Chan et al., 2009, Kılıç et al., 2018, Hakkim et al., 2021, Xiong et al., 2020
C_6H_6O	278.4	Kılıç et al., 2018, Hakkim et al., 2021, Khare et al., 2020
$C_5H_4O_2$	188.2	Hakkim et al., 2021
C_6H_8O	188.2	Kılıç et al., 2018
C_8H_8	83.5	Kılıç et al., 2018, Hakkim et al., 2021, Xiong et al., 2020

C_7H_6O	188.2	Kılıç et. al., 2018
C_8H_{10}	69.4	Chan et al., 2009, Kılıç et al., 2018, Hakkim et al., 2021, Xiong et al., 2020
$C_6H_6O_2$	229.4	Kılıç et al., 2018
C_9H_{10}	188.2	Kılıç et al., 2018
C_9H_{12}	75.3	Chan et al., 2009, Kılıç et al., 2018, Hakkim et al., 2021, Xiong et al., 2020
C_9H_{14}	117.6	Kılıç et al., 2018
$C_7H_8O_2$	200	Yee et al., 2013
$C_{10}H_8$	185	Chan et. al., 2009, Kılıç et al., 2018, Hakkim et al., 2021, Khare et al., 2020
$C_{10}H_{12}$	129.4	Kılıç et al., 2018, Khare et al., 2020
$C_{10}H_{14}$	86.3	Kılıç et al., 2018, Hakkim et al., 2021, Khare et al., 2020
$C_{10}H_{16}$	176.5	Xiong et al., 2020
$C_{11}H_{10}$	221.6	Chan et al., 2009, Kılıç et al., 2018, Khare et al., 2020
$C_{11}H_{12}$	88.2	Khare et al., 2020
$C_6H_4Cl_2$	9.4	Xiong et al., 2020
$C_{11}H_{14}$	102.9	Kılıç et al., 2018, Khare et al., 2020
$C_{10}H_{12}O$	70.6	Khare et al., 2020
$C_{10}H_{16}O$	2.5	Khare et al., 2020
$C_{10}H_{18}O$	0.9	Khare et al., 2020
$C_{12}H_{12}$	176.5	Chan et al., 2009, Khare et al., 2020
$C_{12}H_{16}$	114.7	Kılıç et al., 2018, Khare et al., 2020
$C_{13}H_{18}$	147.1	Khare et al., 2020
$C_{10}H_8O_3$	170.6	Khare et al., 2020
$C_{13}H_{20}$	147.1	Khare et al., 2020
$C_{13}H_{22}$	4.6	Khare et al., 2020
$C_{14}H_{14}$	288.2	Khare et al., 2020
$C_{10}H_{16}O_3$	35.3	Witkowski et al., 2017
$C_{14}H_{18}$	194.1	Khare et al., 2020
$C_{14}H_{20}$	194.1	Khare et al., 2020
$C_{14}H_{22}$	194.1	Khare et al., 2020
$C_{16}H_{24}$	252.9	Khare et al., 2020
$C_{17}H_{28}$	276.5	Khare et al., 2020
$C_{18}H_{30}$	305.9	Khare et al., 2020

Table S4: Correlation table (R) for the 11 factors with independent tracer species.

Tracer Species	Cooking	Solvents	Road Construction	Biogenic	Petrol 4-Wheeler	Paddy	Heating & Waste Burning	Petrol 2-Wheeler	Industrial	Photo-chemical	CNG
WS	-0.4	-0.2	-0.1	0.1	-0.3	-0.2	-0.2	-0.2	-0.3	0.0	-0.2
WD	0.1	-0.1	0.2	0.1	0.0	0.1	0.2	0.1	-0.1	0.1	0.1
CO_2	0.2	0.2	0.1	-0.3	**0.7**	0.4	0.4	**0.7**	**0.8**	-0.1	0.3
N_2O	0.0	0.0	-0.1	-0.1	0.2	0.0	0.1	0.2	0.4	-0.1	0.2
CH_4	0.2	0.3	0.0	-0.3	**0.6**	0.4	0.3	**0.6**	**0.8**	-0.1	0.3
PM_{10}	0.3	0.2	0.1	-0.2	0.4	**0.7**	**0.7**	0.5	0.5	0.0	0.3
$PM_{2.5}$	0.3	0.2	0.1	-0.3	0.3	**0.7**	**0.6**	0.4	0.5	0.0	0.2
CO	0.3	0.3	0.1	-0.2	**0.7**	0.5	0.5	**0.6**	**0.7**	-0.1	0.4

NO	0.1	0.2	0.0	-0.2	**0.8**	0.3	0.4	0.5	**0.7**	-0.1	0.3
NO_2	0.1	0.1	0.1	-0.2	0.3	0.3	**0.7**	0.4	0.2	0.0	0.2
NO_x	0.1	0.2	0.0	-0.2	**0.8**	0.3	0.5	**0.6**	**0.7**	-0.1	0.3
O_3	0.1	-0.1	0.3	0.5	-0.2	0.0	-0.1	-0.2	-0.3	0.4	-0.2
SO_2	0.0	-0.1	-0.2	-0.1	0.2	0.3	0.4	0.2	0.2	0.0	0.2
AT	0.2	-0.1	0.2	**0.7**	-0.2	-0.3	**-0.6**	-0.3	-0.4	0.3	0.1
RH	-0.1	0.1	-0.2	-0.5	0.0	-0.2	-0.4	-0.1	0.2	-0.4	-0.1
PAR	0.2	-0.2	0.2	**0.7**	-0.2	-0.1	-0.2	-0.3	-0.3	0.3	-0.2
VC	-0.2	-0.2	0.1	**0.6**	-0.3	-0.2	-0.3	-0.3	-0.4	0.2	-0.2
FC	0.4	0.3	0.2	-0.3	0.3	**0.8**	**0.6**	0.5	0.4	0.3	0.3
HD	-0.2	-0.3	-0.3	-0.4	-0.1	0.3	**0.8**	0.1	-0.1	0.0	0.1

AT: Ambient Temperature, RH: Relative Humidity, PAR: Photosynthetic active radiation, VC: Ventilation Coefficient, FC: Daily Fire Count, HD: Heating Demand

Table S5: Emissions from different sectors for north-western, south-western, and south-eastern fetch regions.

VOC (Gg y^{-1})									
	NW			**SW**			**SE**		
Sector	**EDGAR**	**REAS**	**FINN**	**EDGAR**	**REAS**	**FINN**	**EDGAR**	**REAS**	**FINN**
Residential fuel usage	764	353	-	1421	947	-	1196	862	-
Industrial	302	113	-	867	55	-	635	133	-
Agricultural Residue	135	0	760	204	0	801	171	0	207
Transport	84	212	-	154	378	-	96	266	-
Solvents	403	78	-	939	222	-	896	204	-
Power Industry	7	2	-	27	4	-	12	4	
$PM_{2.5}$ (Gg y^{-1})									
Sector	**NW**			**SW**			**SE**		
Residential fuel usage	382	379	-	713	934	-	597	830	-
Industrial	158	173	-	524	541	-	342	307	-
Agricultural Residue	97	0	95	206	0	100	168	0	26

Transport	8	65	-	18	137	-	12	80	-
Solvents	0	0	-	0	0	-	0	0	-
Power Industry	144	14	-	453	68	-	215	61	-
PM_{10} (Gg y^{-1})									
Sector	**NW**			**SW**			**SE**		
Residential fuel usage	750	401	-	1391	994	-	1157	882	-
Industrial	211	308	-	684	1015		458	539	-
Agricultural Residue	103	0	192	217	0	203	177	0	52
Transport	10	67	-	22	140	-	14	83	-
Solvents	0	0	-	0	0	-	0	0	-
Power Industry	213	28	-	679	130		321	118	

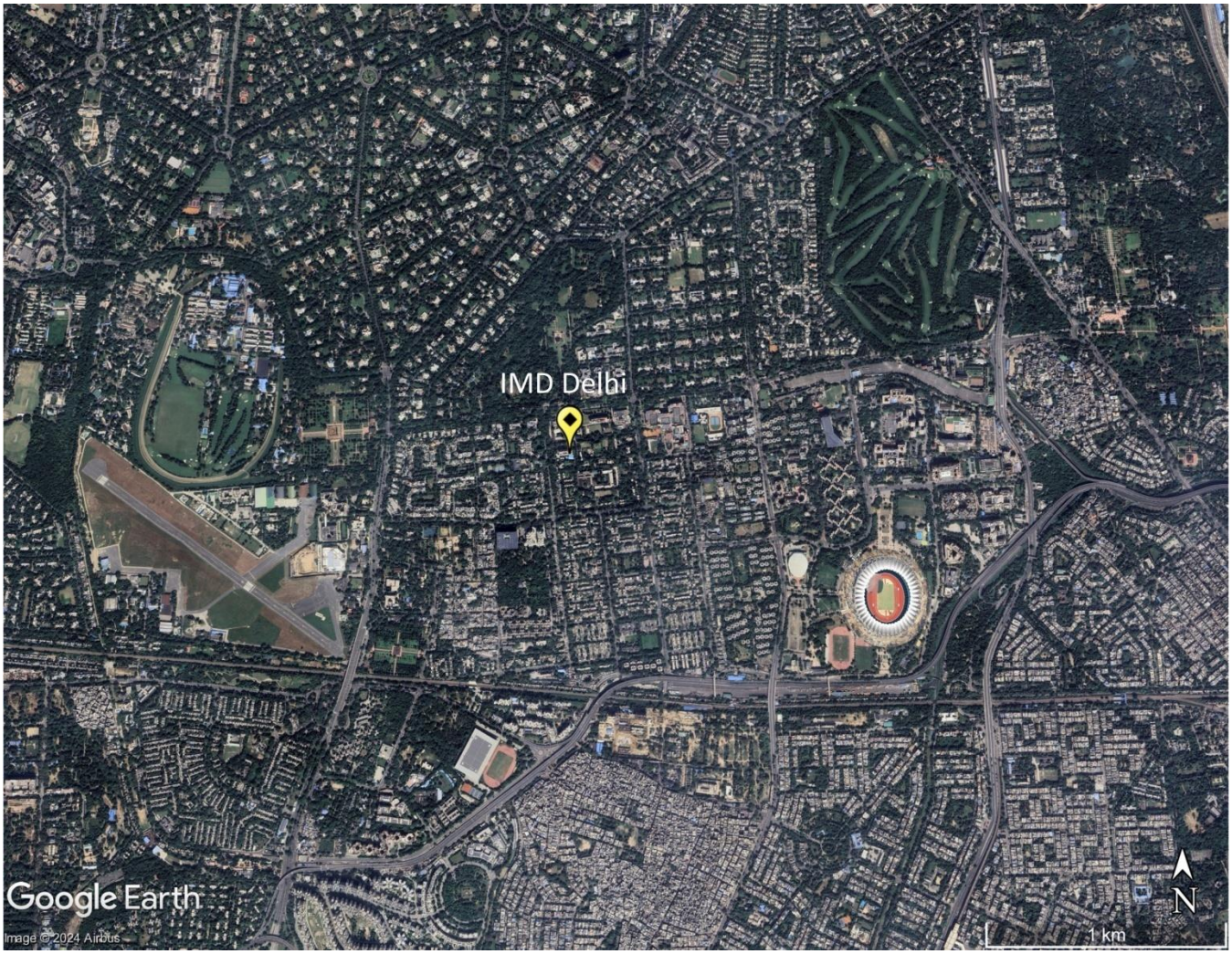

Figure S1: Map of the immediate surroundings of the IMD (28.5896°N-77.2210°E) sampling site in Central Delhi. (Google Earth Imagery ©Google Earth)

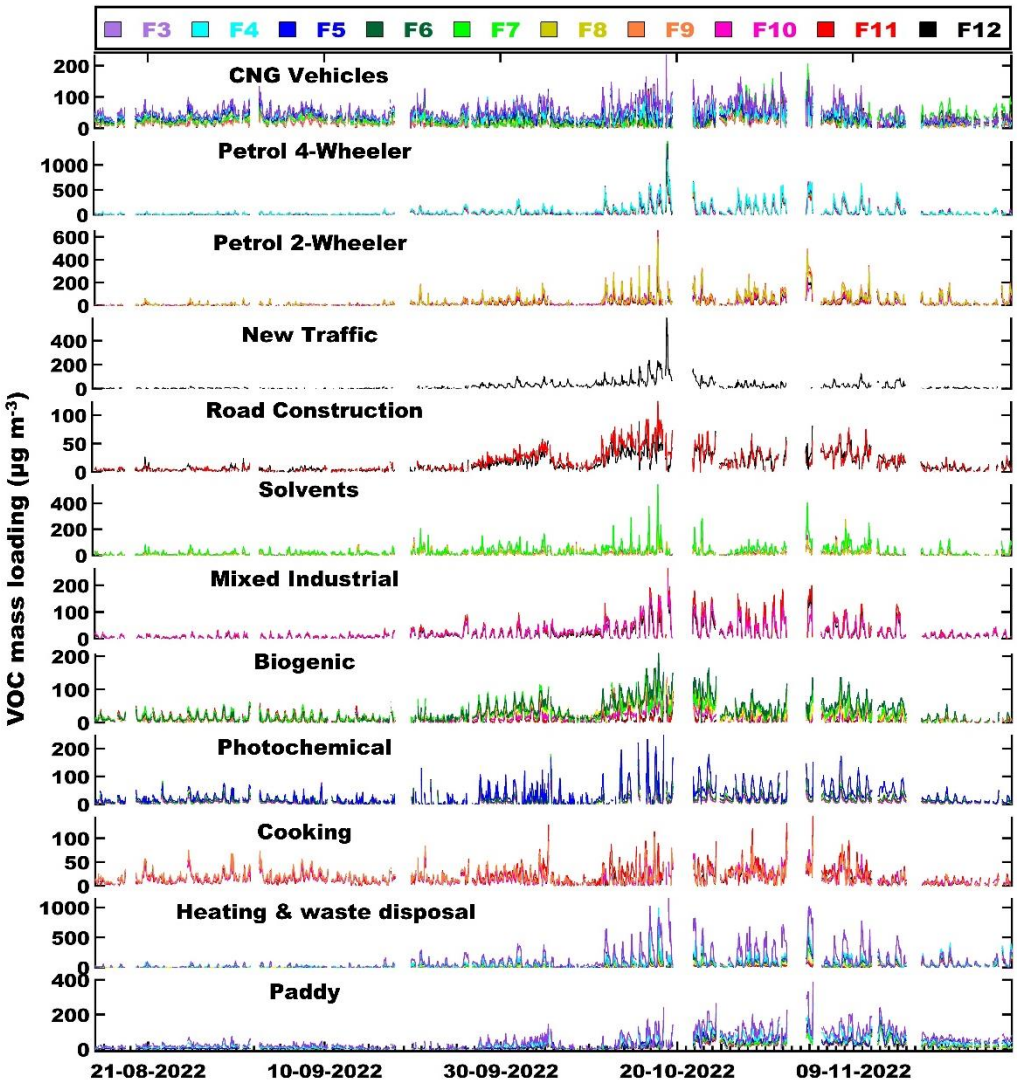

Figure S2: Evolution of the factor contribution time series when the number of factors is increased from 3 to 12.

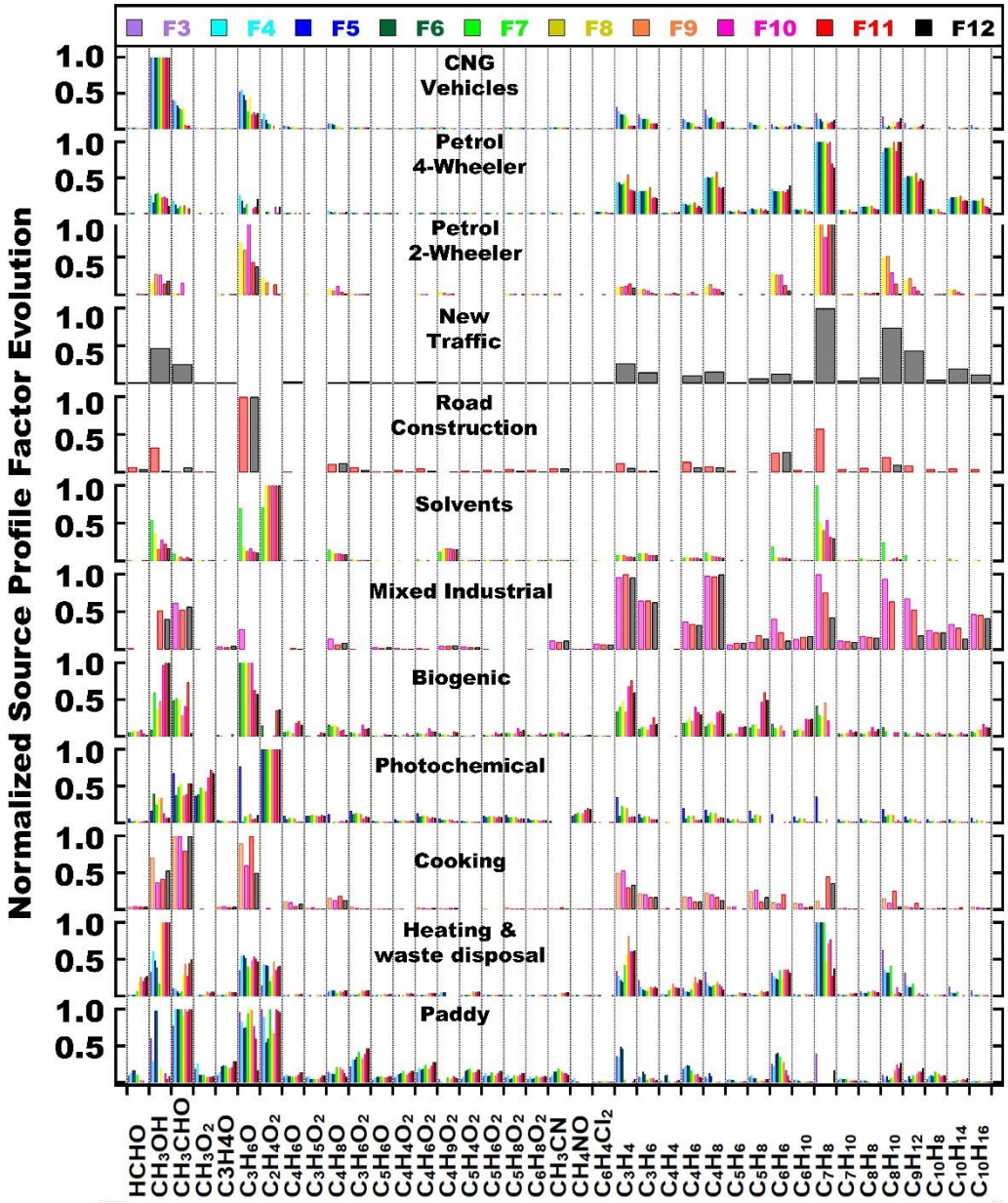

Figure S3: Evolution of the normalized PMF factor profile when the number of factors is increased from 3 to 12.

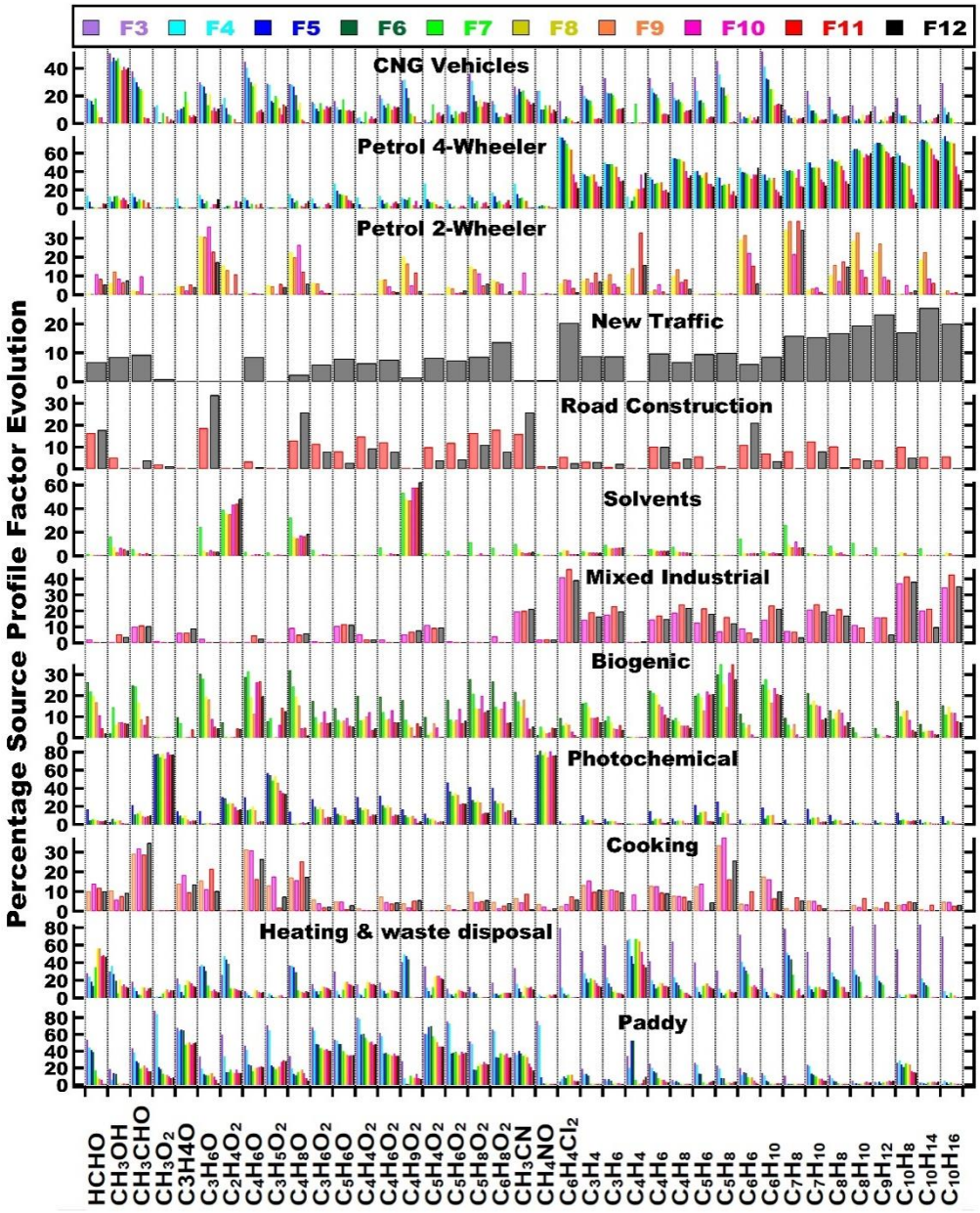

Figure S4: Evolution of the percentage of the mass explained by different sources when the number of factors is increased from 3 to 12.

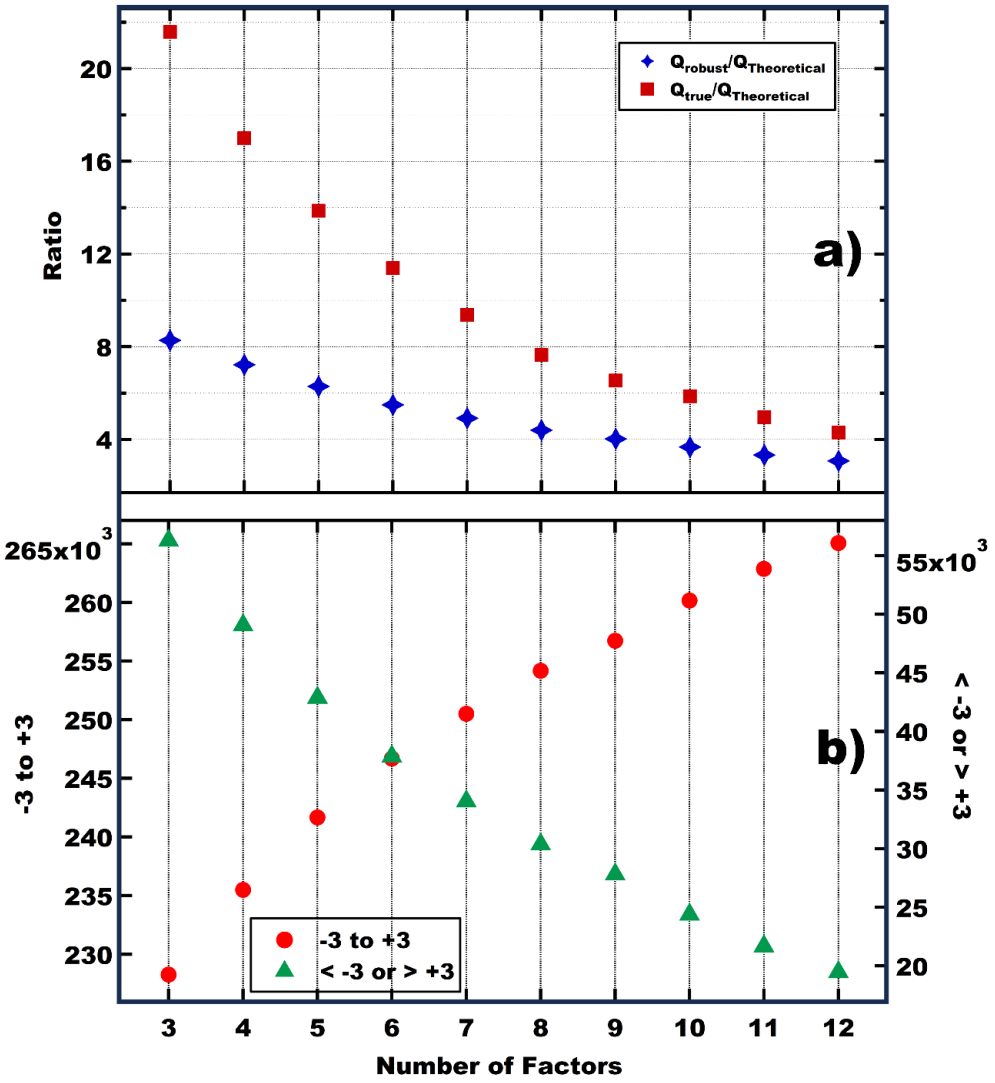

Figure S5: represents change in the a) $Q_{true}/Q_{theoretical}$ ratio and $Q_{robust}/Q_{theoretical}$, b) scaled residuals beyond 3 standard deviations and under 3 standard deviations when the number of factors is increased from 3 to 12.

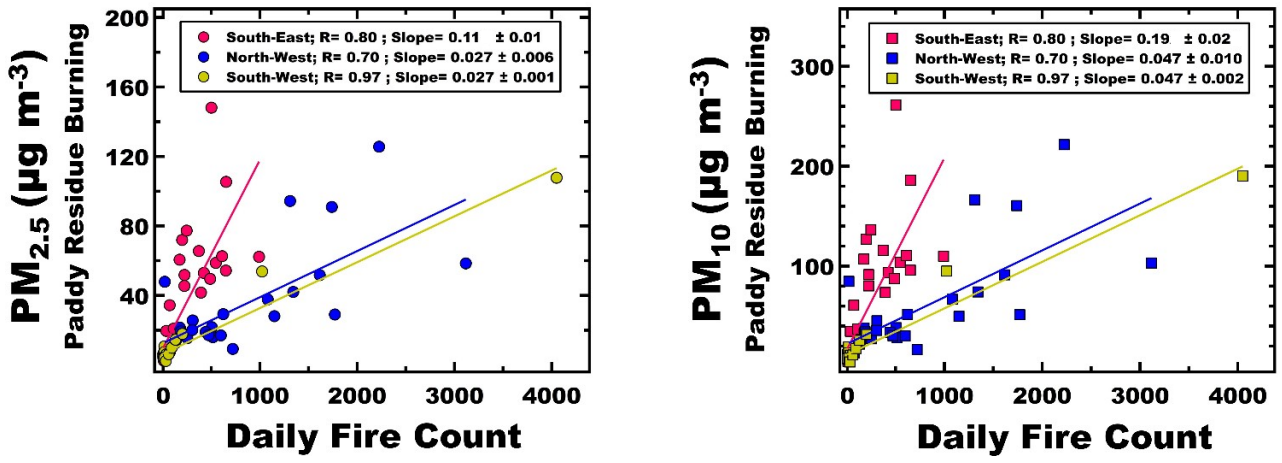

Figure S6: Cross correlation analysis of $PM_{2.5}$ and PM_{10} mass loadings from the paddy residue burning factor at the receptor site with the 24-hour averaged fire count in three fetch regions (SE, NW, SW).

Figure S7 Photographs of complete burning practises that prevail over Punjab. Fires of complete burns tend to be larger than fires from partial burns (Figure S8) and suffer lower omission error during satellite detection. Photo credits: Pooja Chaudhary and Vinayak Sinha

Figure S8 Photographs of partial burning practises that prevail in peri-urban areas and in the eastern IGP. The left-hand side shows a line burn of residue left behind by the combined harvester while the right-hand side shows a heap burn of residue next to the threshing machine after manual harvest. Fires of partial burns tend to be very small in comparison to the 375 x 375 m satellite footprint and suffer from close to 100% omission error during satellite detection. Photo credits: Pooja Chaudhary

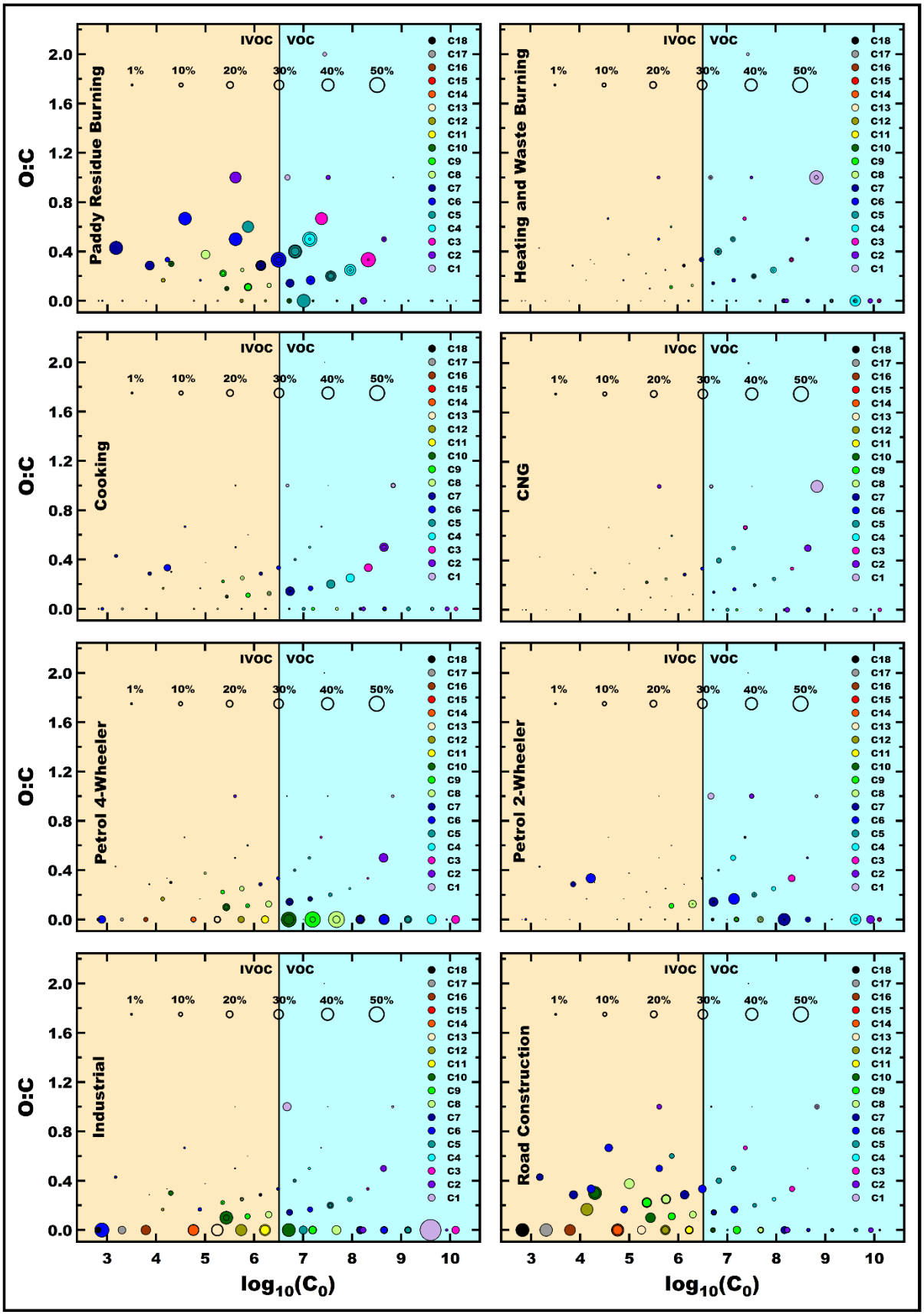

Figure S9: Volatility oxidation state plots for all factors that individually contribute more than 3% to the total SOA formation potential.

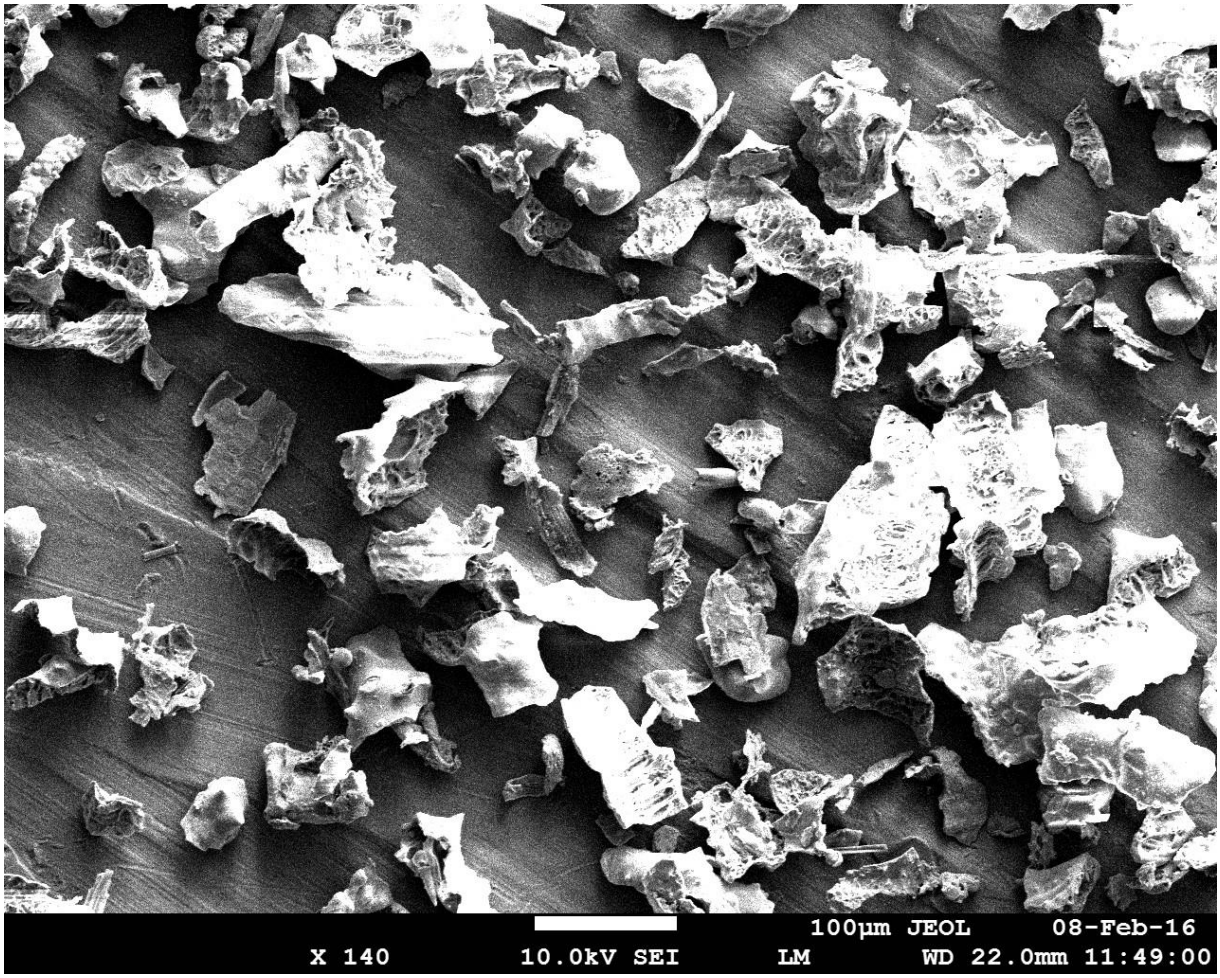

Figure S10 SEM image of rice ash from the electrostatic precipitator of an industrial boiler fired with rice husk and straw illustrating the coarse mode nature of the ash generated during the combustion of phytolith containing biomass.

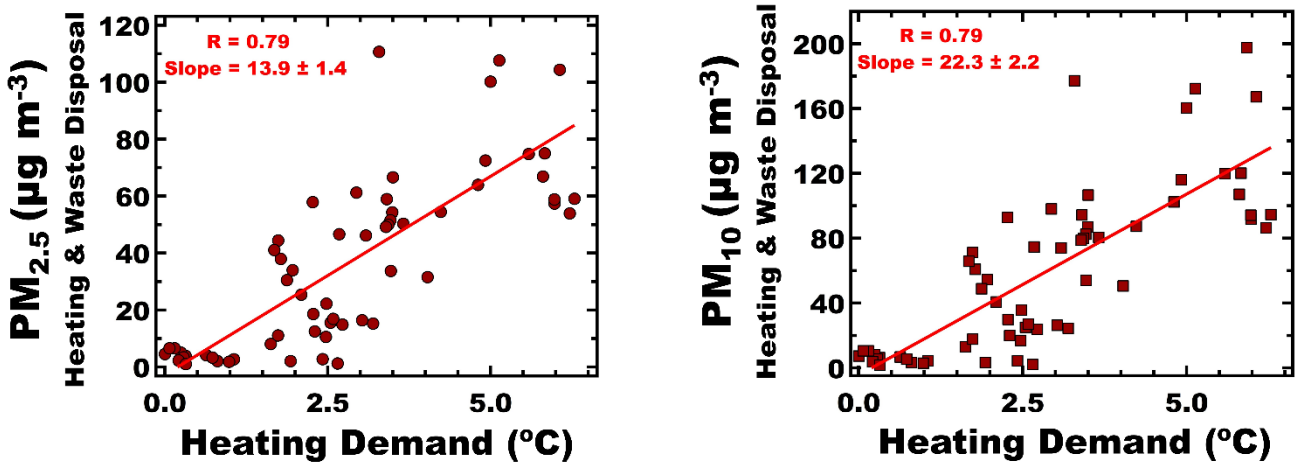

Figure S11:Cross correlation analysis of the $PM_{2.5}$ and PM_{10} mass loadings attributed to residential heating and waste burning at the receptor site with the 24-hour averaged heating demand

Figure S12: Random selection of photographs clicked while driving around Delhi. One can clearly see the white CNG cylinders mounted in the place where the fuel tank used to be during vehicle conversion. Photo credits: Kriti Annika Sinha

References:

Bruns, E. A., Slowik, J. G., El Haddad, I., Kilic, D., Klein, F., Dommen, J., Temime-Roussel, B., Marchand, N., Baltensperger, U., and Prévôt, A. S. H.: Characterization of gas-phase organics using proton transfer reaction time-of-flight mass spectrometry: Fresh and aged residential wood combustion emissions. Atmos. Chem. Phys., 17(1), 705–720, https://doi.org/10.5194/acp-17-705-2017, 2017.

Camredon, M., Hamilton, J. F., Alam, M. S., Wyche, K. P., Carr, T., White, I. R., Monks, P. S., Rickard, A. R., and Bloss, W. J.: Distribution of gaseous and particulate organic composition during dark α-pinene ozonolysis, Atmos. Chem. Phys., 10, 2893–2917, https://doi.org/10.5194/acp-10-2893-2010, 2010.

Chan, A. W. H., Kautzman, K. E., Chhabra, P. S., Surratt, J. D., Chan, M. N., Crounse, J. D., Kürten, A., Wennberg, P. O., Flagan, R. C., and Seinfeld, J. H.: Secondary organic aerosol formation from photooxidation of naphthalene and alkylnaphthalenes: implications for oxidation of intermediate volatility organic compounds (IVOCs), Atmos. Chem. Phys., 9, 3049–3060, https://doi.org/10.5194/acp-9-3049-2009, 2009.

Chandra, B. P., and Sinha, V.: Contribution of post-harvest agricultural paddy residue fires in the N.W. Indo-Gangetic Plain to ambient carcinogenic benzenoids, toxic isocyanic acid and carbon monoxide. Environ. Int., 88, 187–197, https://doi.org/10.1016/J.ENVINT.2015.12.025, 2016.

Coggon, M. M., Lim, C. Y., Koss, A. R., Sekimoto, K., Yuan, B., Gilman, J. B., Hagan, D. H., Selimovic, V., Zarzana, K. J., Brown, S. S., Roberts, J. M., Müller, M., Yokelson, R., Wisthaler, A., Krechmer, J. E., Jimenez, J. L., Cappa, C., Kroll, J. H., De Gouw, J., and Warneke, C.: OH chemistry of non-methane organic gases (NMOGs) emitted from laboratory and ambient biomass burning smoke: evaluating the influence of furans and oxygenated aromatics on ozone and secondary NMOG formation. Atmos. Chem. Phys, 19, 14875–14899, https://doi.org/10.5194/acp-19-14875-2019, 2019.

Derwent, R. G., Jenkin, M. E., Saunders, S. M., and Pilling, M. J.: Photochemical ozone creation potentials for organic compounds in northwest Europe calculated with a master chemical mechanism. Atmos. Environ., 32(14–15), 2429–2441, https://doi.org/10.1016/S1352-2310(98)00053-3, 1998.

Derwent, R. G., Jenkin, M. E., Utembe, S. R., Shallcross, D. E., Murrells, T. P., and Passant, N. R.: Secondary organic aerosol formation from a large number of reactive man-made organic compounds. Sci. Total. Environ., 408(16), 3374–3381, https://doi.org/10.1016/J.SCITOTENV.2010.04.013, 2010.

Fleming, L. T., Weltman, R., Yadav, A., Edwards, R. D., Arora, N. K., Pillarisetti, A., Meinardi, S., Smith, K. R., Blake, D. R., and Nizkorodov, S. A.: Emissions from village cookstoves in Haryana, India, and their potential impacts on air quality, Atmos. Chem. Phys., 18, 15169–15182, https://doi.org/10.5194/acp-18-15169-2018, 2018.

Fukusaki, Y., Kousa, Y., Umehara, M., Ishida, M., Sato, R., Otagiri, K., Hoshi, J., Nudejima, C., Takahashi, K., and Nakai, S.: Source region identification and source apportionment of volatile organic compounds in the Tokyo Bay coastal area, Japan. Atmos. Environ.: X, 9, https://doi.org/10.1016/j.aeaoa.2021.100103, 2021.

Gkatzelis, G. I., Hohaus, T., Tillmann, R., Gensch, I., Müller, M., Eichler, P., Xu, K.-M., Schlag, P., Schmitt, S. H., Yu, Z., Wegener, R., Kaminski, M., Holzinger, R., Wisthaler, A., and Kiendler-Scharr, A.: Gas-to-particle partitioning of major biogenic oxidation products: a study on freshly formed and aged biogenic SOA, Atmos. Chem. Phys., 18, 12969–12989, https://doi.org/10.5194/acp-18-12969-2018, 2018.

Guenther, A., Karl, T., Harley, P., Wiedinmyer, C., Palmer, P. I., and Geron, C.: Estimates of global terrestrial isoprene emissions using MEGAN (Model of Emissions of Gases and Aerosols from Nature). Atmos. Chem. Phys., 6(11), 3181–3210, https://doi.org/10.5194/ACP-6-3181-2006, 2006.

Haeri, F.: Molecular Speciation of Organic Nitrogen Compounds Separated in Smoke Particles Emitted from Burning Western U.S. Wildland Fuels, PhD thesis, Carnegie Mellon University, Pittsburgh, PA, USA, https://doi.org/10.1184/R1/22670578.v1, 2023.

Hakkim, H., Kumar, A., Annadate, S., Sinha, B., and Sinha, V.: RTEII: A new high-resolution (0.1° × 0.1°) road transport emission inventory for India of 74 speciated NMVOCs, CO, NOx, NH3, CH4, CO2, PM2.5 reveals massive overestimation of NOx and CO and missing nitromethane emissions by existing inventories. Atmos. Environ.: X, 11, 100118, https://doi.org/10.1016/J.AEAOA.2021.100118, 2021.

Harrison, M. A., Barra, S., Borghesi, D., Vione, D., Arsene, C., and Olariu, R. I.: Nitrated phenols in the atmosphere: a review. Atmos. Environ., 39(2), 231-248, https://doi.org/10.1016/j.atmosenv.2004.09.044, 2005.

Hatch, L. E., Luo, W., Pankow, J. F., Yokelson, R. J., Stockwell, C. E., and Barsant K. C.: Identification and quantification of gaseous organic compounds emitted from biomass burning using two-dimensional gas chromatography–time-of-flight mass spectrometry. Atmos. Chem. Phys., 15, 1865–1899, https://doi.org/ https://doi.org/10.5194/acp-15-1865-2015, 2015.

Hatch, L. E., Yokelson, R. J., Stockwell, C. E., Veres, P. R., Simpson, I. J., Blake, D. R., Orlando, J. J., and Barsanti K. C.: Multi-instrument comparison and compilation of non-methane organic gas emissions from biomass burning and implications for smoke-derived secondary organic aerosol precursors. Atmos. Chem. Phys., 17, 1471–1489, https://doi.org/10.5194/acp-17-1471-2017, 2017.

Hsu, C. Y., Wu, P. Y., Chen, Y. C., Chen, P. C., Guo, Y. L., Lin, Y. J., and Lin, P.: An integrated strategy by using long-term monitoring data to identify volatile organic compounds of high concern near petrochemical industrial parks. Sci. Total. Environ., 821, https://doi.org/10.1016/j.scitotenv.2022.153345, 2022.

Jordan, C., Fitz, E., Hagan, T., Sive, B., Frinak, E., Haase, K., Cottrell, L., Buckley, S., and Talbot, R.: Long-term study of VOCs measured with PTR-MS at a rural site in New Hampshire with urban influences. Atmos. Chem. Phys., 9(14), 4677–4697, https://doi.org/10.5194/ACP-9-4677-2009, 2009.

Kamarulzaman, N. H., Le-Minh, N., and Stuetz, R. M.: Identification of VOCs from natural rubber by different headspace techniques coupled using GC-MS. Talanta, 191, 535-544, https://doi.org/10.1016/j.talanta.2018.09.019, 2019.

Khare, P., Machesky, J., Soto, R. He, M., Presto, A. A. and Gentner, D. R.: Asphalt-related emissions are a major missing nontraditional source of secondary organic aerosol precursors. Science Advances 6, eabb9785, https://doi.org/10.1126/sciadv.abb9785, 2020.

Kılıç, D., El Haddad, I., Brem, B. T., Bruns, E., Bozetti, C., Corbin, J., Durdina, L., Huang, R.-J., Jiang, J., Klein, F., Lavi, A., Pieber, S. M., Rindlisbacher, T., Rudich, Y., Slowik, J. G., Wang, J., Baltensperger, U., and Prévôt, A. S. H.: Identification of secondary aerosol precursors emitted by an aircraft turbofan, Atmos. Chem. Phys., 18, 7379–7391, https://doi.org/10.5194/acp-18-7379-2018, 2018.

Koss, A. R., Sekimoto, K., Gilman, J. B., Selimovic, V., Coggon, M. M., Zarzana, K. J., Yuan, B., Lerner, B. M., Brown, S. S., Jimenez, J. L., Krechmer, J., Roberts, J. M., Warneke, C., Yokelson, R. J., and De Gouw, J.: Non-methane organic gas emissions from biomass burning: Identification, quantification, and emission factors from PTR-ToF during the FIREX 2016 laboratory experiment. Atmos. Chem. Phys., 18(5), 3299–3319, https://doi.org/10.5194/ACP-18-3299-2018, 2018.

Kumar, A., Hakkim, H., Sinha, B., and Sinha, V.: Gridded 1 km × 1 km emission inventory for paddy stubble burning emissions over north-west India constrained by measured emission factors of 77 VOCs and district-wise crop yield data. Sci. Total. Environ., 789, 148064, https://doi.org/10.1016/J.SCITOTENV.2021.148064, 2021.

Kumar, A., Sinha, V., Shabin, M., Hakkim, H., Bonsang, B., and Gros, V.: Non-methane hydrocarbon (NMHC) fingerprints of major urban and agricultural emission sources for use in source apportionment studies. Atmos. Chem. Phys., 20(20), 12133–12152, https://doi.org/10.5194/ACP-20-12133-2020, 2020.

Lignell, H., Epstein, S. A., Marvin, M. R., Shemesh, D., Gerber, B., and Nizkorodov, S.: Experimental and Theoretical Study of Aqueous cis-Pinonic Acid Photolysis. J. Phys. Chem. A 2013, 117, 12930−12945, https://doi.org/10.1021/jp4093018, 2013.

Loubet, B., Buysse, P., Gonzaga-Gomez, L., Lafouge, F., Ciuraru, R., Decuq, C., Kammer, J., Bsaibes, S., Boissard, C., Durand, B., Gueudet, J.-C., Fanucci, O., Zurfluh, O., Abis, L., Zannoni, N., Truong, F., Baisnée, D., Sarda-Estève, R., Staudt, M., and Gros, V.: Volatile organic compound fluxes over a winter wheat field by PTR-Qi-TOF-MS and eddy covariance, Atmos. Chem. Phys. 22, 2817–2842, https://doi.org/10.5194/acp-22-2817-2022, 2022.

Mochizuki, T., Kawamura, K., Miyazaki, Y., Kunwar, B., and Boreddy, S. K. R.: Distributions and sources of low-molecular-weight monocarboxylic acids in gas and particles from a deciduous broadleaf forest in northern Japan. Atmos. Chem. Phys., 19(4), 2421-2432, https://doi.org/10.5194/acp-19-2421-2019, 2019.

Nowakowska, M., Herbinet, O., Dufour, A., and Glaude, P. A.: Kinetic Study of the Pyrolysis and Oxidation of Guaiacol. J. Phys. Chem. A. A, 122(39), 7894–7909, https://doi.org/10.1021/acs.jpca.8b06301, 2018.

Palm, B., Peng, Q., Fredrickson, C. D., Lee B. H, Garofalo, L. A., Pothier, M. A., Kreidenweis S. M., Farmer D. K., Pokhrel, R. P., Shen, Y., Murphy S. M., Permar W., Hu L. Campos T.L., Hall S. R., Ullmann K., Zhang, X., Flocke, F., Fischer, E. V., and Thornton, J. A.: Quantification of organic aerosol and brown carbon evolution in fresh wildfire plumes. P. Natl. Acad. Sci. USA, 117 (47) 29469-29477, https://doi.org/10.1073/pnas.2012218117, 2020.

Ramasamy, S., Nakayama, T., Imamura, T., Morino, Y., Kajii, Y. and Sato, K.: Investigation of dark condition nitrate radical- and ozone-initiated aging of toluene secondary organic aerosol: Importance of nitrate radical reactions with phenolic products. Atmos. Environ. 219, 117049, https://doi.org/10.1016/j.atmosenv.2019.117049, 2019.

Sarkar, C., Sinha, V., Kumar, V., Rupakheti, M., Panday, A., Mahata, K. S., Rupakheti, D., Kathayat, B., and Lawrence, M. G.: Overview of VOC emissions and chemistry from PTR-TOFMS measurements during the SusKat-ABC campaign: high acetaldehyde, isoprene and isocyanic acid in wintertime air of the Kathmandu Valley. Atmos. Chem. Phys., 16, 3979–4003, https://doi.org/10.5194/acp-16-3979-2016, 2016.

Sarkar, C., Sinha, V., Sinha, B., Panday, A. K., Rupakheti, M., and Lawrence, M. G.: Source apportionment of NMVOCs in the Kathmandu Valley during the SusKat-ABC international field campaign using positive matrix factorization. Atmos. Chem. Phys., 17(13), 8129–8156, https://doi.org/10.5194/ACP-17-8129-2017, 2017.

Stockwell, C. E., Veres, P. R., Williams, J., and Yokelson, R. J.: Characterization of biomass burning emissions from cooking fires, peat, crop residue, and other fuels with high-resolution proton-transfer-reaction time-of-flight mass spectrometry. Atmos. Chem. Phys., 15, 845–865, https://doi.org/ https://doi.org/10.5194/acp-15-845-2015, 2015.

Toda, K., Obata, T., Obokin, V. A., Potemkin, V. L., Hirota, K., Takeuchi, M., Arita, S., Khodzher, T. V., and Grachev, M. A.: Atmospheric methanethiol emitted from a pulp and paper plant on the shore of Lake Baikal, Atmos. Environ., 44, 2427–2433, https://doi:10.1016/j.atmosenv.2010.03.037, 2010.

Wang, Z., Yuan, B., Ye, C., Roberts, J., Wisthaler, A., Lin, Y., Li, T., Wu, C., Peng, Y., Wang, C., Wang, S., Yang, S., Wang, B., Qi, J., Wang, C., Song, W., Hu, W., Wang, X., Xu, W., … Shao, M.: High Concentrations of Atmospheric Isocyanic Acid (HNCO) Produced from Secondary Sources in China. Environ. Sci. Technol., 54(19), 11818–11826, https://doi.org/10.1021/acs.est.0c02843, 2020.

Wang, M., Wang, Q., Ho, S. S. H., Li, H., Zhang, R., Ran, W., Que, L.: Chemical characteristics and sources of nitrogen-containing organic compounds at a regional site in the North China Plain during the transition period of autumn and winter. Sci. Total. Environ., 812, 151451, https://doi.org/10.1016/j.scitotenv.2021.151451, 2022.

Witkowski, B., and Gierczak, T.: cis-Pinonic acid oxidation by hydroxyl radicals in the aqueous phase under acidic and basic conditions: kinetics and mechanism. Environ. Sci. Technol., 51(17), 9765-9773, https://doi.org/10.1021/acs.est.7b02427, 2017.

Xing, C., Wan, Y., Wang, Q., Kong, S., Huang, X., Ge, X., Xie, M. and Yu, H.: Molecular characterization of brown carbon chromophores in atmospherically relevant samples and their gas-particle distribution and diurnal variation in the atmosphere. J. Geophys Res-Atmos., 128, e2022JD038142, https://doi.org/10.1029/2022JD038142, 2023.

Xiong, Y., Zhou, J., Xing, Z., and Du, K.: Optimization of a volatile organic compound control strategy in an oil industry center in Canada by evaluating ozone and secondary organic aerosol formation potential. Environ. Res., 191, 110217, https://doi.org/10.1016/j.envres.2020.110217, 2020.

Xu, C., GaoL., Lyu, C., Qiao, L. Huang, D., Liu, Y., Li, D. and Zheng, M.: Molecular characteristics, sources and environmental risk of aromatic compounds in particulate matter during COVID-2019: Nontarget screening by ultra-high resolution mass spectrometry and comprehensive two-dimensional gas chromatography. Environ. Int., 167 107421, https://doi.org/10.1016/j.envint.2022.107421, 2022.

Yáñez-Serrano, A. M., Filella, I., LLusià, J., Gargallo-Garriga, A., Granda, V., Bourtsoukidis, E., Williams, J., Seco, R., Cappellin, L., Werner, C., de Gouw, J., and Peñuelas, J.: GLOVOCS - Master compound assignment guide for proton transfer reaction mass spectrometry users. Atmos. Environ., 244, 117929, https://doi.org/10.1016/J.ATMOSENV.2020.117929, 2021.

Yao, L., Wang, M.-Y., Wang, X. -K. Liu, Y.-J., Chen, H.-F., Zheng, J., Nie, W., Ding, A.-J., Geng, F.-H., Wang, D.-F., Chen, J.-M., Worsnop, D. R. and Wang, L.: Detection of atmospheric gaseous amines and amides by a high-resolution time-of-flight chemical ionization mass spectrometer with protonatedethanol reagent ions. Atmos. Chem. Phys., 16, 14527–14543. https://doi.org/10.5194/acp-16-14527-2016, 2016.

Zaytsev, A., Koss, A. R., Breitenlechner, M., Krechmer, J. M., Nihill, K. j. Lim, C. Y., Rowe, J. C., Cox, J. L., Moss, J., Roscioli, J. R., Canagaratna, M. R., Worsnop, D. R., Kroll, J. H., and Keutsch1, F. N.: Mechanistic Study of Formation of Ring-retaining and Ring-opening Products from Oxidation of Aromatic Compounds under Urban Atmospheric Conditions. Atmos. Chem. Phys., 19, 15117–15129, https://doi.org/10.5194/acp-19-15117-2019, 2019.